# Aluminum Phthalocyanine Tetrasulfonate in MCF-10F, Human Breast Epithelial Cells: A Hole Burning Study

Nebojsa Milanovich, Tonu Reinot, John M. Hayes, and Gerald J. Small
Ames Laboratory-USDOE and Department of Chemistry, Iowa State University, Ames, Iowa 50011 USA

ABSTRACT Laser-induced holes are burned in the absorption spectrum of aluminum phthalocyanine tetrasulfonate (APT) in MCF-10F, human breast epithelial cells. The hole burning mechanism is shown to be nonphotochemical. The fluorescence excitation spectra and hole spectra are compared with those of APT in hyperquenched glassy films of water, ethanol, and methanol. The results show that the APT is in an acidic, aqueous environment with a hydrogen-bonded network similar to that of glassy water, but showing the influence of other cellular components. Pressure shifts of holes allow the local compressibility about the APT to be determined.

## INTRODUCTION

Biological samples when subjected to cryogenic temperatures display an inherent disorder that gives these samples glasslike properties. Thus high-resolution optical techniques such as fluorescence line narrowing (FLN) (Jankowiak and Small, 1991) and hole burning (Jankowiak and Small, 1993), which have been developed to probe the inhomogeneously broadened absorption spectra of impurity molecules in glasses, are increasingly being used to investigate biological samples. FLN, for example, has been used to study DNA-carcinogen complexes at physiological damage levels (Jankowiak et al., 1988; Ariese et al., 1996) and protein-chromophore interactions (Kaposi et al., 1993). Hole burning has been used extensively to study electron and energy transfer processes in photosynthetic systems (Jankowiak and Small, 1993; Reddy et al., 1992; Small, 1995). Because the bandwidths obtained by these techniques are so narrow compared with room temperature absorption widths, Stark shifts and broadening (Kador et al., 1987; Meixner et al., 1986) and pressure effects (Chang et al., 1995; Gafert et al., 1993; Gradl et al., 1991; Reddy et al. 1995; Schellenberg et al., 1994; Sesselman et al., 1987; Wu et al., 1996; Zollfrank et al., 1991) on the spectra can be accurately measured.

In this paper we report the results of hole burning and pressure shifts for a dye molecule within cultured mammalian cells. The results reported here represent the first measurements of hole burning and compressibility for dye molecules within intact cells. The hole burning mechanism will be shown to be nonphotochemical hole burning (NPHB), which occurs because of rearrangement of the matrix solvating the dye rather than photochemistry of the dye itself. The mechanisms and properties of NPHB have been extensively studied both by us (Jankowiak and Small, 1993; Hayes et al., 1987; Jankowiak and Small, 1987) and by others (Moerner, 1987), and NPHB properties have been shown to be extremely sensitive to the molecular environment of the dye molecule (Reinot et al., 1997a; Milanovich et al., 1996). The demonstration in this paper of NPHB of a dye molecule within cells opens up the possibility of utilizing hole burning, with organelle-specific dye molecules to "image" anomalies in subcellular structures. As differences in hole burning parameters such as hole width and hole growth kinetics are related to differences in $T_2$ optical relaxation, whereas hole shifts with pressure and temperature are determined by short-range solvent forces, hole burning imaging is directly analogous to magnetic resonance imaging, which measures proton $T_1$ relaxation times to detect differences in tissue structures.

Application of hole burning to a cellular system requires careful selection of an appropriate dye molecule that can be detected within the cell. In choosing a dye, certain important biological and spectroscopic criteria must be satisfied. First, the probe molecule used must be membrane permeable. Second, autofluorescence caused by other biomolecules inside the cell may have spectra that interfere with the probe molecule's spectrum. In mammalian cells, such as those used in this study, autofluorescence is caused primarily by flavin coenzymes (flavin adenine dinucleotide (FAD) and flavin mononucleotide (FMN); absorbance wavelength/emission wavelength (abs./em.) ~450/515 nm) (Benson et al., 1979) and reduced pyridine nucleotides (NADH, abs./em. ~340/460 nm) (Aubin, 1979). In addition, the presence of the pH indicator phenol red (abs./em. 560/578.4 nm, pH ~7.4, at room temperature and 77 K, respectively), used in culture media, may also interfere with the probe molecule's spectra. Interference from autofluorescence and phenol red fluorescence suggests that a dye absorbing and fluorescing at wavelengths greater than 600 nm would be best suited for hole burning. In general, longer wavelengths will penetrate tissues better than shorter wavelengths. Third, the dye should be dispersed throughout the cell without undergoing a chemical reaction. Finally, the dye molecule must be capable of being induced to burn a hole in the spectrum, i.e., it must be in a disordered environment and have sufficient

*Received for publication 3 November 1997 and in final form 20 January 1998.*

Address reprint requests to Dr. John M. Hayes, Ames Laboratory–USDOE, Iowa State University, Ames, IA 50011. Tel.: 515-294-4872; Fax: 515-294-1699; E-mail: jmhayes@iastate.edu.



0006-3495/98/05/2680/09 $2.00

coupling to the environment that electronic excitation will trigger solvent rearrangement, and it must be photochemically stable and not aggregate.

In choosing an appropriate dye molecule, we considered photosensitizers used in photodynamic therapy (PDT). PDT is a cancer treatment method based on photooxidation of intracellular biomolecules of the targeted cells initiated by a photosensitized dye molecule (Henderson and Dougherty, 1992). What makes these photosensitizers ideal is that cells are able to take up these molecules. Many photosensitizers have been considered for use as photodynamic dyes. These dye molecules retain the basic "core" structure of either a porphyrin or a phthalocyanine ring, whereas differences in uptake and biodistribution are determined by the side chains and/or metals associated with the molecule's core (Boyle and Dolphin, 1996). Phthalocyanines, in particular, have absorption maxima in the 670–680-nm range. In the current study we have chosen aluminum phthalocyanine tetrasulfonate (APT) to stain cells in vitro. Although APT is not organelle specific, it has been used as a probe molecule for studying disorder in amorphous water (Reinot et al., 1996, 1997a,b; Kim et al., 1995, 1996), and therefore its hole burning behavior is well characterized. Much work has also been done using APT as a photodynamic dye (Rosenthal, 1991; Spikes, 1986; Moan et al., 1994). Ben-Hur et al. (1987) investigated the uptake of several tetrasulfonated metallophthalocyanines in Chinese hamster cells. They found that of the seven metallophthalocyanines considered, uranyl phthalocyanine tetrasulfonate and APT were taken up at the highest rate and that APT was one of only two metallophthalocyanines not to aggregate under physiological conditions. The authors further add that the dye molecules make their way into the cell first by binding to a cell surface receptor followed by the internalization of the receptor-ligand complex. Confocal laser scanning microscopy of APT in human melanoma cells indicates that the internalized dye molecules can be found in lysosomes (Peng et al., 1991).

We report here the hole burning of APT inside MCF-10F human mammary epithelial cells (Soule et al., 1990; Tait et al., 1990). The cells were stained with APT, at which time the cells were prepared for study at liquid helium temperatures (~4.5 K). Spectra obtained for APT in MCF-10F cells were compared to those for APT in hyperquenched glassy water, ethanol, and methanol. We also present here the results of pressure effects on the center frequency of holes burned in APT's fluorescence excitation spectrum and, subsequently, determine the compressibility of the dye in MCF-10F cells. In general, we are interested in detecting cellular anomalies so that we might eventually apply NPHB to the early detection of disease.

## EXPERIMENTAL

### Cell culture

MCF-10F human mammary epithelial cells were obtained from the American Type Culture Collection (ATCC). MCF-10F cells were cultured in a 1:1 mixture of Ham's F12 medium and Dulbecco's modified Eagle's medium containing 5% horse serum, 100 ng/ml cholera enterotoxin, 10 $\mu$g/ml insulin, 0.5 $\mu$g/ml hydrocortisol, and 20 ng/ml epithelial growth factor. All cell culture items were purchased from Sigma-Aldrich Chemical Co. (St. Louis, MO). The cells were grown in 25 $cm^2$ culture flasks and incubated at 37°C under an air atmosphere containing 5% $CO_2$; cells were passed weekly.

### Sample preparation

For sample preparation, cells were grown in 75-$cm^2$ culture flasks. Cells were allowed to grow to near confluence, at which time sterile-filtered APT (Porphyrin Products, Login, UT) in phosphate-buffered saline (PBS) was added to the culture flasks. Final APT concentration in the culture flasks was adjusted to $10^{-4}$ M. Samples were then incubated overnight (18–19 h) at 37°C under a 5% $CO_2$ atmosphere. After incubation the culture media containing excess APT were removed from the flasks, and the cells were washed three times with PBS to remove excess dye and media. Washed cells were detached from the flasks by treating the cells with trypsin. After trypsin treatment the appropriate culture medium was added to each flask with trypsin (1:1), and the cell population was determined with a Coulter Multisizer II cell counter. Typical cell populations ranged from $1 \times 10^6$ to $3 \times 10^6$ cells/ml. Samples were then centrifuged for 5 min at $100 \times g$, and the resulting supernatant was discarded. The cells were resuspended in freezing medium, which consisted of culture medium with 5% dimethyl sulfoxide. Aliquots of these samples were mixed with glycerol (1:1) and transferred to 5 mm o.d. gelatin capsules. Final samples typically contained between $\sim 10^5$ and $3 \times 10^5$ cells. Because a cryopreservative was used (dimethyl sulfoxide), the samples were slow-cooled to −70°C in a styrofoam box inside a freezer overnight to avoid ice formation in the cells at cryogenic temperatures (Farrant et al., 1977; Franks, 1977).

### Cell viability

Stained MCF-10F cells were tested for viability with a Coulter EPICS XL-MCL flow cytometer. A frozen sample, as prepared above, was rapidly thawed and stained with propidium iodide (PI) (Molecular Probes, Eugene, OR). Cell viability was determined by PI uptake. Nonviable cells are able to take up the dye, whereas viable cells are not. Typically, viability was >90%, and almost no debris resulting from ruptured cells was present.

### High-pressure system

Pressures used in this study were attained with standard gas cylinder pressures, and helium gas was used as the pressure-transmitting medium. Gas pressure applied to the sample was manually regulated by a model E11-8-N115H two-stage pressure regulator (Air Products, Des Moines, IA). In line with the pressure regulator was a PX945-3KGI pressure

transducer (0–20.7 MPa detection range with 0.1% accuracy) and a model DP941-E pressure readout (both from Omega Engineering, Stamford, CT). Stainless steel tubing (316, I.D. ⅛″) was used to connect the cylinder regulator and pressure transducer. A reducing union reduced the tubing diameter to 1⁄16″. The 1⁄16″ gas delivery line was connected at the head of the sample holder with a bulkhead union. Inside the cryostat head, 1⁄16″ tubing connected to the other end of the bulkhead union was wrapped along the length of the sampleholder's shaft for thermal grounding. A male connector joined the gas delivery line to the high-pressure cell. All connectors were Swagelok®.

The high pressure cell is made of copper with a horizontal cross section of 1⅛″ × 1⅛″ and a height of 2″. The schematic in Fig. 1 is a vertical cross section of the cell. Windows made of antireflection coated BK7 glass (⅛″ thickness, ½″ diameter) (Melles Griot, Irvine, CA) on three of the cell's four vertical sides provided optical access to the sample. Windows were glued to window mounts with low-temperature epoxy (Janis Research Co., Wilmington, MA), and the window mounts were then secured to the cell body. An O-ring made of indium metal provided the seal between the window mount and the cell body.

In an experiment, a single sample contained in the above-described gelatin capsule was placed inside the precooled (−70°C) high-pressure cell. After the sample was placed inside the cell, the male connector mentioned above was screwed into place. One-inch copper spacers were placed between the mounting plate of the sample holder and cell to allow for easy connection of the delivery line with the cell. At low temperatures (<40 K), gases inside the pressure delivery line, i.e., oxygen and nitrogen from air, solidify and prevent the delivery of gas pressure to the sample. Therefore, the delivery line was continuously flushed with helium as the cell and delivery line were being connected. Consequently, a small pressure remained inside the cell (~100 kPa) until the cell was inserted into a precooled (~4.5 K) cryostat (Supertran continuous flow cryostat; Janis Research Co.), at which time the pressure was decreased to ambient pressure (defined as 0 kPa). That the delivery line was unobstructed was checked by allowing the cell to cool to ~4.5 K and applying between 30 and 70 kPa of pressure to the cell. Temperature rose rapidly by 1–3 K if the delivery line was not obstructed, at which time pressure was dropped to ambient and the temperature returned to ~4.5 K. Temperature of the sample was monitored with a silicon diode (model DT-470; Lakeshore Cryogenics, Westerville, OH) in direct contact with the high-pressure cell.

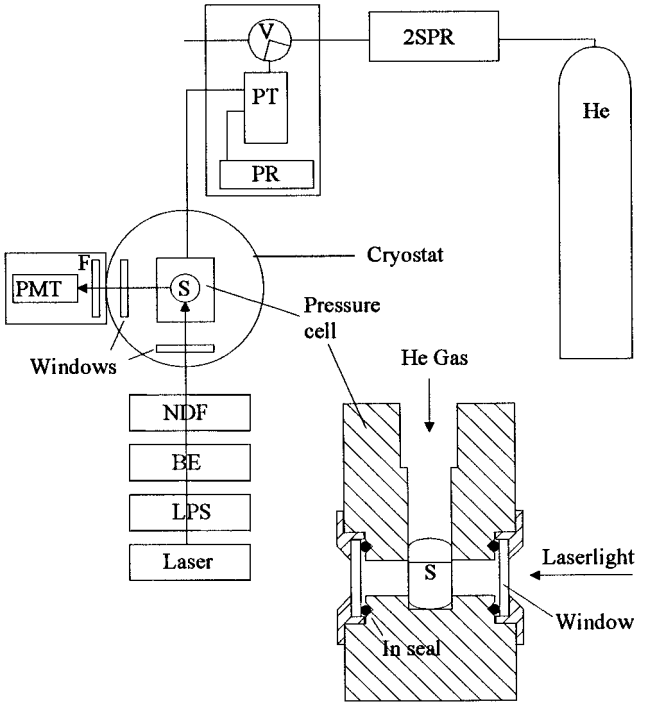


FIGURE 1 Schematic representation of experimental apparatus showing details of the high-pressure system. S, sample; NDF, neutral density filter; BE, beam expander; LPS, laser power stabilizer; PMT, photomultiplier tube; F, filter; PR, pressure readout; PT, pressure transducer; V, valve; 2SPR, two-stage pressure regulator; He, helium gas cylinder.

## Laser system

The fluorescence excitation system used has previously been described (Kim et al., 1995, 1996). Briefly, a Coherent Innova 90-6 argon ion laser (Coherent, Santa Clara, CA) was used to pump a CR-699-29 ring dye laser, using DCM special laser dye (Exciton, Dayton, OH). This dye gives 100–600 mW power over a wavelength region of 610–700 nm. Laser intensity was stabilized with an LS100 laser power stabilizer (Cambridge Research and Instrumentation, Cambridge, MA), and subsequently the laser beam was expanded with a telescope. The laser was operated in two modes: broad-range continuous scanning without intracavity etalons, and short-range scanning with intracavity etalons. The scanning ranges and linewidths for the broad scanning mode and short-range mode were 1000 $cm^{-1}$ and 0.4 $cm^{-1}$, and 10 $cm^{-1}$ and <30 MHz (0.001 $cm^{-1}$), respectively.

Hole burning and scanning intensities were varied by using a series of neutral density (absorption) filters. Laser beam intensities used for detection were chosen so as not to further alter the spectra. The estimated change in fractional hole depths at each wavelength was less than 0.0005 for channel time $t = 0.2$ s and intensity $I = 60$ nW/cm$^2$ (see Fig. 4, where the burn intensity is 1.7 $\mu$W/cm$^2$). For kinetics curve detection, burn intensities less than 2 $\mu$W/cm$^2$ were used, while a decrease in the fluorescence signal was concurrently recorded. Because the fluorescence signal decreases very rapidly during the first few seconds of burning, and much slower later, the typical channel time in the beginning was 0.1 s. After approximately half of the burn was completed, the channel time was changed to 1 s.

The fluorescence excitation signal was collected with a GaAs photomultiplier tube (PMT) and photon counter (SR-400; Stanford Research, Sunnyvale, CA). The excitation

signal was filtered from the PMT with cutoff filters at 750 nm. The laser was scanned and data were collected with a PC.

## RESULTS AND DISCUSSION

The fluorescence excitation spectrum of APT-treated MCF-10F cells at 4.5 K is shown in Fig. 2. The figure also shows the fluorescence excitation spectra of APT in freezing media, in hyperquenched glassy water, and in glassy ethanol. Comparing the spectra of APT in freezing media with that in cells, it is apparent that there is a large shift in the fluorescence excitation maxima of the spectra in the former, and the spectrum is considerably broader than that in cells. These differences between the freezing media spectrum and the spectrum in cells are conclusive evidence that the APT in the cellular samples is associated with the cells rather than simply dissolved in the suspension medium. The width of the freezing media spectrum indicates that there is a wide variety of environments in which the APT can be found, whereas in cells or in single component glasses the APT environment is less inhomogeneous. In previous work on NPHB of APT in glassy samples (Reinot et al., 1996, 1997a,b; Kim et al., 1995, 1996), it was shown that the fluorescence maximum is solvent and pH dependent. In hyperquenched glassy water, the APT fluorescence shifts red with increasing pH. At pH 3.4, e.g., the maximum is at 672 nm, at 668 nm for neutral pH (as shown in Fig. 2), and at 663 nm for pH 11.6. Relative to neutral hyperquenched glassy water, the fluorescence excitation maximum also shifts red in glassy ethanol (679 nm) or methanol (677 nm) (Reinot et al., 1997a). A water content of ~1% has shifted the fluorescence excitation maximum given in Fig. 2 for ethanol to 677 nm. Along with the changes in peak position, there are also changes in the fluorescence band shape that occur in the different glassy solvents. As can be seen in Fig. 2, for the cellular samples and for hyperquenched glassy water, the fluorescence excitation band is very broad, with a nearly flat-topped peak. In previous work (Reinot et al., 1997a; Kim et al., 1995) it has been shown that there are two bands contributing to the absorption. Similar structure is also observed in ethanol and methanol, where the bands are somewhat better resolved (Reinot et al., 1997a). In Fig. 2 the spectra for ethanol and freezing media clearly show two peaks, whereas the two bands are poorly resolved in water and the cell spectra. The nature of the second band has not been conclusively determined, although it does not seem to be a vibronic absorption band. From hole burning action spectra in glassy water, ethanol, and methanol (Reinot et al., 1997a), it appears to be an APT configuration that rapidly converts to the lower energy absorbing band from which the fluorescence originates. This is evidenced by the broadening and lower saturated fractional hole depth of holes burned on the blue side of the absorption relative to holes burned on the red side. In hyperquenched glassy water, the hole widths for the bluer holes indicate that a ~1-ps relaxation process is involved. The red side holes, on the other hand, have widths that depend on the annealing of the sample. In samples annealed at temperatures near the glass transition temperature, the hole widths are as narrow as 110 MHz at 5.0 K, i.e., they approach the fluorescence lifetime; in unannealed samples they are ~500 MHz (Kim et al., 1996). In comparing the fluorescence excitation spectra of APT in cells with that in the glassy media, the peak position and band shape for APT-treated cells indicate a low pH, aqueous environment. Studies of APT as a photodynamic agent have shown that APT is present in lysosomes (Peng et al., 1991). Lysosomes are subcellular structures whose function is macromolecular digestion (Alberts et al., 1994). The digestive enzymes present in lysosomes are acid hydrolases that function best in a low pH environment. That APT is localized in lysosomes is consistent with the spectral observations of Fig. 2. That the environment is similar to hyperquenched glassy water will be further demonstrated in what follows.

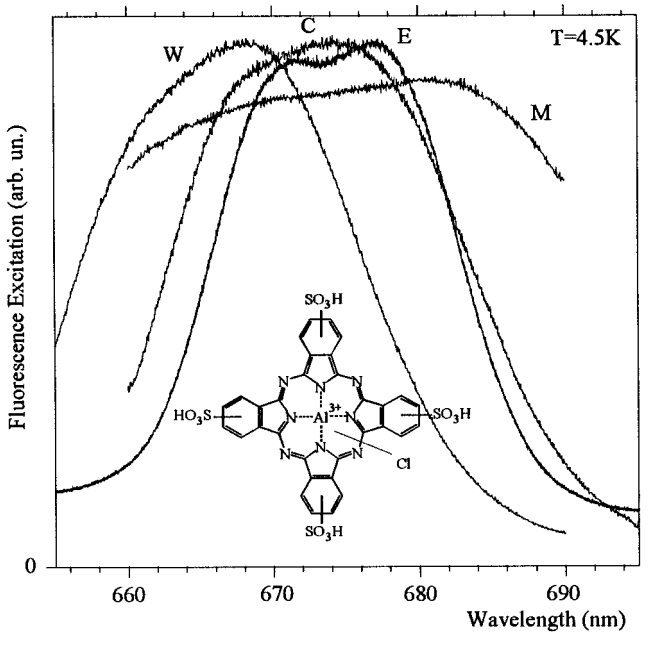


FIGURE 2 Fluorescence excitation spectra of APT in various glassy matrices. The curves are W, water ($\lambda_{max}$ = 668.2 nm); C, MCF-10F cells in 1:1 freezing medium and glycerol ($\lambda_{max}$ = 675.4 nm); E, ethanol ($\lambda_{max}$ = 676.9 nm); M, 1:1 freezing medium and glycerol ($\lambda_{max}$ = 681.3 nm). The structure of APT is shown in the lower portion of the figure.

Fig. 3 shows typical hole spectra for APT-treated cells at 4.5 K after burning at a burn frequency, $\omega_B$ = 14,771 $cm^{-1}$. For the lowest burn fluence, a zero-phonon hole with a width of ~1500 MHz is observed. As shown in the figure, continued burning leads to saturation and broadening of the zero-phonon hole, growth of a phonon side band hole with a peak at $\omega_B$ − 31 ± 2 $cm^{-1}$, and development of weak vibronic hole structure. Two conclusions regarding hole burning of APT in cells can be drawn from the data shown in Fig. 3. First, that hole burning of APT in cells is observed is strong evidence that the APT is in a glassy environment, as hole burning is either absent or much reduced in crystalline environments (Reinot et al.,

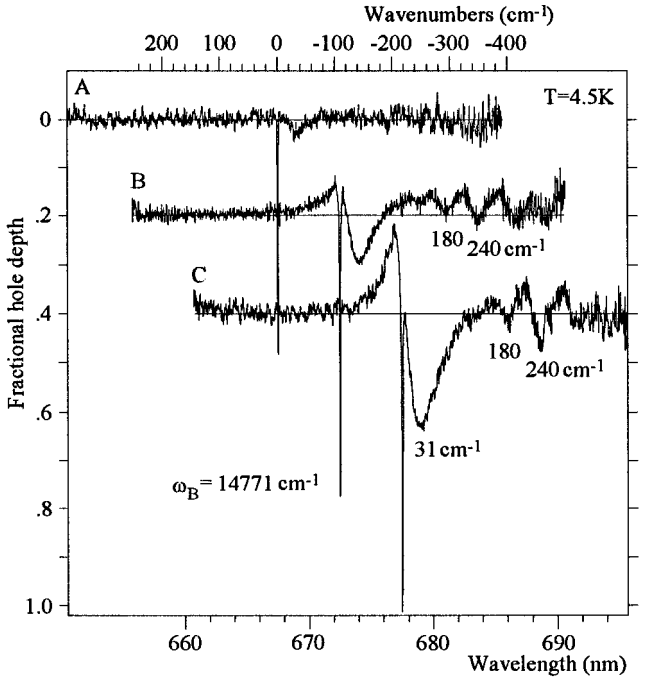


FIGURE 3 Hole profiles for holes burned at $\omega_B$ = 14,771 $cm^{-1}$ with increasing fluence. Burn fluences were (*A*) 0.086 $J/cm^2$, (*B*) 0.81 $J/cm^2$, and (*C*) 7.3 $J/cm^2$. All three spectra show a phonon side band hole with a mean phonon frequency of 31 $cm^{-1}$. Spectra *B* and *C* also show pseudovibronic holes at 180 $cm^{-1}$ and 240 $cm^{-1}$. For clarity, *B* and *C* were shifted relative to *A*. Shifts were 5 nm, 0.2, and 10 nm, 0.4 for *B* and *C*, respectively.

1997a; Kim et al., 1995). Second, from the spectral hole profile shown in Fig. 3, the hole burning most likely occurs through a nonphotochemical hole burning process. NPHB is widely observed in glasses and is due to a configurational rearrangement of solvent molecules around an electronically excited probe molecule. The presence of a broad distribution of nearly isoenergetic structural configurations is a universal property of glasses that arises from their disordered nature. A characteristic of NPHB is that the "product" absorption (antihole) lies within the original inhomogeneously broadened absorption band and, for $\pi$-$\pi^*$ transitions is blue-shifted relative to $\omega_B$, as is shown for APT in cells in Fig. 3. The blue-shifted antihole has been explained in terms of an increase in glass free volume in the vicinity of the probe molecule (Shu and Small, 1990, 1992a).

It is interesting to compare the hole burning results for APT in cells with the results for APT in hyperquenched glassy water, ethanol, and methanol (Reinot et al., 1997a,b; Kim et al., 1995). APT in hyperquenched glassy water is a highly efficient hole burning system with hole widths as narrow as 110 MHz when burned at 4.5 K after annealing at temperatures near the glass transition temperature. Even in unannealed films, the hole widths are typically only ~500 MHz. In ethanol and methanol, hole burning at 4.5 K of films annealed at higher temperatures gave widths of 1500 MHz and 2000 MHz, respectively. The phonon sideband holes observed for APT in hyperquenched glassy water are peaked at 38 $cm^{-1}$ compared with 26 $cm^{-1}$ for ethanol and 17 $cm^{-1}$ for methanol. The phonon frequencies for hyperquenched glassy water are considerably higher than the 20–25-$cm^{-1}$ phonon sideband holes observed for a wide variety of other hole burning systems. Given the slow cooling to −70°C used for the cellular samples, it is appropriate to compare the characteristics of holes for APT in cells with the characteristics for the annealed films. For the cell samples, the zero-phonon hole widths are more similar to ethanol than to hyperquenched glassy water, whereas the mean phonon frequency (~31 $cm^{-1}$) is between that for ethanol (26 $cm^{-1}$) and hyperquenched glassy water (38 $cm^{-1}$). The point is not that APT is in an alcoholic environment, but rather that the disordered hydrogen bond structure, which gives hyperquenched glassy water its unique properties as a hole burning host (Reinot et al., 1997b), is preserved in cells, although it is somewhat modified by the other cellular components.

One can also compare the Huang-Rhys factors, *S*, for APT in the various glasses. The Huang-Rhys factor is a measure of the electron-phonon coupling strength and, at low temperatures, determines the saturated zero-phonon hole depth, because at any frequency within the inhomogeneously broadened origin band, the zero-phonon contribution to absorption will be exp[$-S$]. From Fig. 3, the fractional hole depth is 0.57, which corresponds to an *S* of 0.56. However, this value must be considered an upper limit for *S*, as the zero-phonon hole is not completely saturated and there is some interference between the zero-phonon hole and the antihole that is evident in the figure. *S* can also be determined by extrapolating the ratio of integrated zero-phonon hole area to the total integrated hole area (zero-phonon hole + phonon side band hole) to zero fluence. This ratio is given by exp[$-2S$] (Jankowiak and Small, 1993; Hayes et al., 1988). Using this method, $S = 0.34$ was determined for APT in cells. *S* was also determined from the kinetic fits discussed later, where $S = 0.36$ was determined. Given that zero-phonon hole depth is measured directly from the kinetics curves, 0.36 can be considered the most accurate value for *S*. Although there is some disparity between the various determinations of *S*, the values are all less than 1.0, indicating that the electron-phonon coupling may be characterized as weak. For APT in annealed hyperquenched glassy water, ethanol, and methanol, *S* values of 0.55, 0.43, and 0.36 were determined (Reinot et al., 1996, 1997a). Thus the value in cells is similar to that observed in the other three systems.

The efficiency of hole burning for APT in hyperquenched glassy water can be judged by the fluence required to burn a 10% hole at 5 K, 0.13 $\mu J\ cm^{-2}$. For APT in MCF-10F cells, a fluence of 6.0 $\mu J\ cm^{-2}$ is needed to burn a 10% hole at $\omega_B$ = 680.9 nm. Thus, although APT-treated cells show fluorescence excitation spectra similar to those observed for APT in hyperquenched glassy water, there are significant differences between the hole burning properties of the two systems. APT in hyperquenched glassy water is more efficient, with narrower zero-phonon holes and a higher frequency phonon side band hole. These results indicate that

there must be a difference between the environment of APT in hyperquenched glassy water and that in lysosomes.

The kinetics of hole burning for APT in cells and in hyperquenched glassy water are also quite different, as shown in Fig. 4. This figure shows, on a logarithmic time scale, the time development of holes in the two systems. For both, the nonexponential hole burning is evidence that the kinetics cannot be described by a single rate. Treating the kinetics as being described by a Gaussian distribution of rates has been successful for a variety of glassy samples (Kenney et al., 1990; Shu and Small, 1992b). In this treatment, the time-dependent fractional hole depth, $D(t)$, is given as

$$D(t) = (2\pi)^{-1/2}\int_{-\infty}^{\infty} dx \exp[-x^2/2]\exp[-\Sigma_0\xi(x)t] \quad (1)$$

where $\Sigma_0 = P\sigma\Omega_0\tau$, and $P$ is the burn photon flux; $\sigma$ is the peak absorption cross section; $\tau$ is the excited state lifetime; and $\Omega_0$ describes the average harmonic frequency of the extrinsic two-level systems, $TLS_{ext}$, the glass configurations described by an intermolecular double well potential that are formed by interaction of the probe molecule with the glass. The integration variable $x = (\lambda - \lambda_0)/\sigma_\lambda$ and $\xi(x) = \exp[-2(\lambda_0 - \sigma_\lambda x)]$. $\lambda$ is the tunneling parameter for $TLS_{ext}$. Equation 1 is derived by assuming that $\lambda$ has a Gaussian distribution centered at $\lambda_0$ with a standard deviation $\sigma_\lambda$, and that tunneling is the rate-determining step in the hole burning process. Equation 1 describes the time dependence only of the zero-phonon hole, but it does not take into account the change in hole shape (broadening). As the zero-phonon hole saturates, i.e., as the subpopulation of molecules in exact resonance with the burn frequency is depleted, nonresonant absorption through the wings of Lorentzian zero-phonon lines becomes important. Because of nonresonant absorption and the burning of molecules absorbing through phonon processes, the hole continues to grow. This is the cause of the deviation of the APT in hyperquenched glassy water data at long times in Fig. 4. The data in Fig. 4 were fit to Eq. 1 by using a four-parameter least-squares fit. The four fit parameters, $\lambda_0$; $\sigma_\lambda$; the Huang-Rhys factor, $S$; and the amplitude at $t = 0$ (a technical parameter), were used to obtain the fits in Fig. 4. Values for $\lambda_0$, $\sigma_\lambda$, and $S$ are given in the figure caption. The values for the two systems are quite similar, although $\lambda_0$ is slightly higher for cells than for hyperquenched glassy water. The more rapid hole burning of APT in hyperquenched glassy water is caused entirely by the homogeneous width being a factor of 3 narrower than for APT in cells.

A further difference in APT between cells and hyperquenched glassy water is indicated in Fig. 5. This shows the effect of burning consecutive holes at 1-nm spectral intervals throughout the APT absorption. As is evident in the figure, when these holes are burned beginning at high energies, and each subsequent hole is displaced by 1 nm to a lower energy (i.e., blue to red), a hole action spectrum results. Note that this action spectrum shows that holes are only burned into the low-energy half of the band. As discussed above, attempts to burn holes in the higher energy band are unsuccessful because of rapid relaxation to the

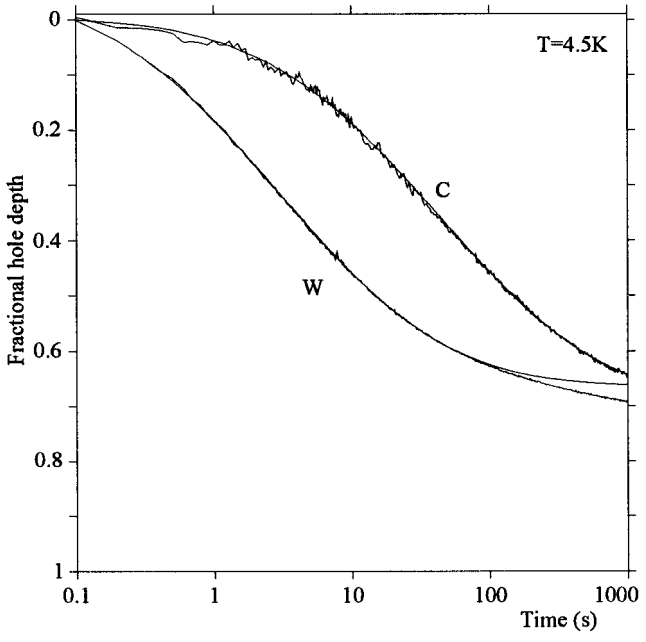


FIGURE 4 Hole growth curves and theoretical fits to Eq. 1 correspond to APT in hyperquenched glassy water (W) and in MCF-10F cells (C). Fit parameters were W: $\lambda_0 = 8.2$, $\sigma_\lambda = 0.99$, $S = 0.40$; C: $\lambda_0 = 9.1$, $\sigma_\lambda = 0.96$, $S = 0.36$. Both curves were for burns using an intensity of 1.7 $\mu W/cm^2$.

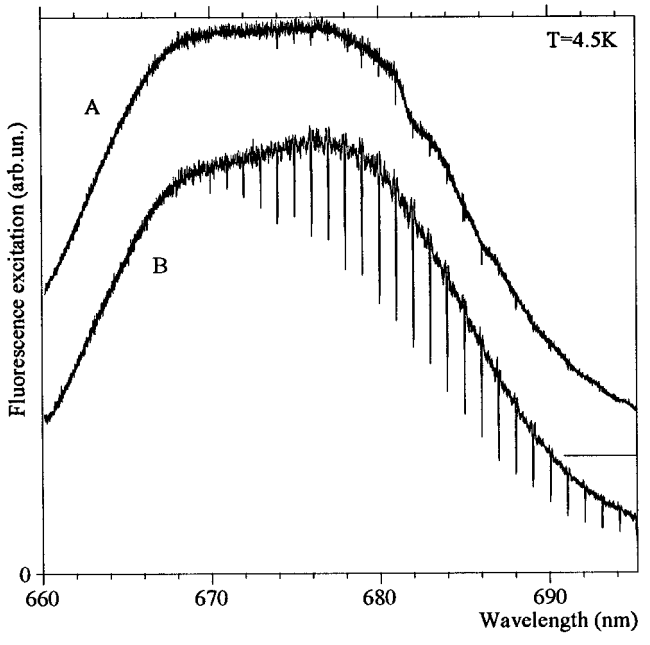


FIGURE 5 Action spectra of holes burned across the fluorescence excitation profile of APT in MCF-10F cells showing the dependence of hole profile on the burn direction. *A* and *B* result from burning holes in the red to blue and blue to red directions, respectively. Each hole was burned using a burn fluence of 133 $mJ/cm^2$.

lower energy band. On the other hand, if the burning is initiated at low energies and subsequent holes are burned to higher energy (i.e., red to blue), hardly any holes result. For APT in hyperquenched glassy water, there is also a dependence on whether the burn proceeds from high to low energy or vice versa, although the result is not as dramatic: there is a diminution of hole depths when burning is from high to low energy, as opposed to the nearly complete absence of holes seen for APT-treated cells. Thus laser-induced hole filling is more efficient for APT in cellular samples than for APT in hyperquenched glassy water. Laser-induced hole filling has previously been discussed (Fearey et al., 1986; Shu and Small, 1992c). The filling was found to be substantially higher when the secondary burn frequency, $\omega_{B2}$, was to higher energy from the initial burn frequency, $\omega_B$. Based on detailed observations of the total spectral changes involved in burning and laser-induced filling, the increased filling efficiency for blue secondary burns was related to the blue-shifted antiholes observed in NPHB (Shu and Small, 1992c). Thus hole filling is due to light-induced antihole reversion. The present observations on laser-induced hole filling of APT in cells are entirely consistent with this filling mechanism. However, a second mechanism involving ~1-ps relaxation from blue-absorbing APT conformers into red-absorbing conformers cannot be ruled out.

A change in the hydrostatic pressure applied to the sample after hole burning affects both the frequency and width of the hole. The frequency shift is linear if the sample is elastic, and is understood to be due to a change in the average equilibrium separation between the solute and the solvent, $r_0$. Therefore, the direction of the frequency shift depends upon both the magnitude and the sign of the pressure change. The frequency shift has been shown to be related to the effect of solvating the probe molecule, i.e., the gas to solvent shift, $(\bar{\nu}_B - \bar{\nu}_{vac})$ and the matrix compressibility, $\kappa$ (Laird and Skinner, 1989):

$$\Delta\bar{\nu}(\bar{\nu}_B \Delta P) = 2\kappa \Delta P(\bar{\nu}_B - \bar{\nu}_{vac}) \qquad (2)$$

Several inferences can be drawn from this expression. First, if $\bar{\nu}_{vac}$ lies within the inhomogeneously broadened absorption band, burning at $\bar{\nu}_{vac}$ will be independent of pressure. Second, the pressure shift is wavelength dependent, increasing as the burn frequency is further removed from $\bar{\nu}_{vac}$. Finally, from the variation of $\Delta\bar{\nu}(\bar{\nu}_B, \Delta P)$ with $\bar{\nu}_B$, one can determine both $\bar{\nu}_{vac}$ and $\kappa$, the compressibility of the sample. The variation in the pressure-induced frequency shift with pressure is shown in Fig. 6. As is evident from the figure, the pressure shift is linear at all burn wavelengths. Therefore, the pressure effects are elastic, although some hole filling does occur, so that the hole shape is not entirely recovered when the pressure is removed. A plot of the slopes of the pressure shifts versus burn frequency can be extrapolated to yield the vacuum absorption frequency of APT. A value of 15,627 $cm^{-1}$ (639.9 nm) was determined. Although this value is consistent with the values determined

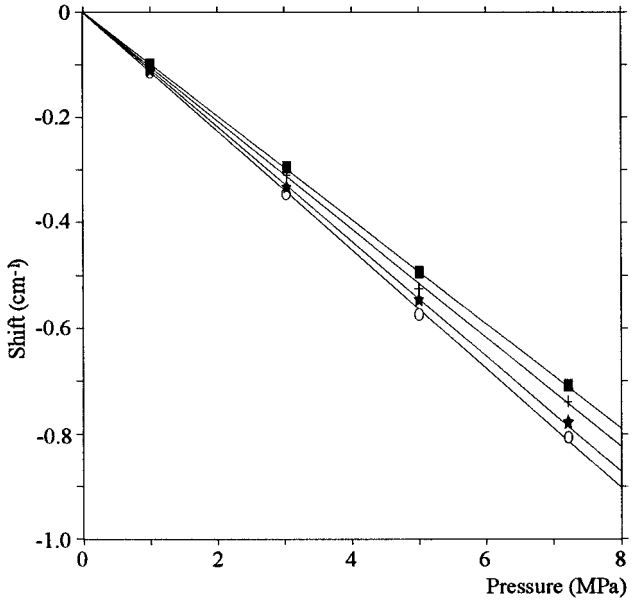


FIGURE 6 Shift of the center frequency for holes burned at 677.5 nm (■), 680.0 nm (+), 682.0 nm (★), and 685.0 nm (○) as a function of hydrostatic pressure.

for similar molecules in a supersonic jet expansion, given the range over which the extrapolation is made, the result is probably accurate to only ~20%. The compressibility determined from Eq. 1 is 0.06 $GPa^{-1}$, which is comparable to the values obtained in a similar manner for organic glasses, polymers, and protein samples (Chang et al., 1995; Gafert et al., 1993; Gradl et al., 1991; Reddy et al., 1995; Schellenberg et al., 1994; Sesselman et al., 1987; Wu et al., 1996; Zollfrank et al., 1991). The question arises: To what does the measured compressibility correspond? For similar measurements on probe molecules within proteins (Schellenberg et al., 1994), the authors argued that the compressibility is of the protein due to the short-range nature ($R^{-6}$) of the interactions causing the pressure shift. If the compressibility being measured is the local compressibility, then the value determined is probably that of the lysosomes in which the dye is located. Experiments in which the lysosomes are disrupted by photoactivation before freezing are planned. It will be of interest to see whether there is any significant difference in compressibility for such samples. Hole burning experiments on a second cell line are also in progress. The cells in these experiments use MCF-7 human breast adenocarcinoma cells. Although the results are still preliminary, there appears to be less reproducibility in these cells, perhaps reflecting the heterogeneity of this cancer cell line (Resnicoff et al., 1987).

The authors thank Kristi Harkins, Paul Kapke, and Donghui Cheng at the ISU Cell and Hybridoma Facility for assistance with cell culture and flow cytometry.

The Ames Laboratory is operated for the U. S. Department of Energy by Iowa State University under contract W-7405-Eng-82, and this work was supported by the Office of Health and Environmental Research, Office of

Energy Research. TR was supported by the Solid State Chemistry and Polymers Program of the Division of Materials Science Division of the National Science Foundation.

## REFERENCES


Alberts, B., D. Bray, J. Lewis, M. Raff, K. Roberts, and J. D. Watson. 1994. *In* Molecular Biology of the Cell. Garland Publishing, New York. 610.

Ariese, F., G. J. Small, and R. Jankowiak. 1996. Conformational studies of depurinating DNA adducts from *syn*-dibenzo[a,l]pyrene diolepoxide. *Carcinogenesis.* 17:829–837.

Aubin, J. E. 1979. Autofluorescence of viable cultured mammalian cells. *J. Histochem. Cytochem.* 27:36–43.

Ben-Hur, E., J. A. Siwecki, H. C. Newman, S. W. Crane, and I. Rosenthal. 1987. Mechanism of uptake of sulfonated metallophthalocyanines by cultured mammalian cells. *Cancer Lett.* 38:215–222.

Benson, R. C., R. A. Meyer, M. E. Zaruba, and G. M. McKhann. 1979. Cellular autofluorescence—is it due to flavins? *J. Histochem. Cytochem.* 27:44–48.

Boyle, R. W., and D. Dolphin. 1996. Structure and biodistribution relationships of photodynamic sensitizers. *Photochem. Photobiol.* 64: 469–485.

Chang, H.-C., R. Jankowiak, N. R. S. Reddy, and G. J. Small. 1995. Pressure dependence of primary charge separation in a photosynthetic reaction center. *Chem. Phys.* 197:307–321.

Farrant, J., C. A. Walter, H. Lee, G. J. Morris, and K. J. Clarke. 1977. Structural and functional aspects of biological freezing techniques. *J. Microsc.* 111:17–34.

Fearey, B. L., T. P. Carter, and G. J. Small. 1986. New studies of non-photochemical holes of dyes and rare-earth ions in polymers. II. Laser-induced hole filling. *Chem. Phys.* 101:279–289.

Franks, F. 1977. Biological freezing and cryofixation. *J. Microsc.* 111: 3–16.

Gafert, J., J. Friedrich, and F. Parak. 1993. A comparative pressure tuning hole burning study of protoporphyrin IX in myoglobin and in a glassy host. *J. Chem. Phys.* 99:2478–2486.

Gradl, G., J. Zollfrank, W. Breinl, and J. Friedrich. 1991. Color effects in pressure-tuned hole-burned spectra. *J. Chem. Phys.* 94:7619–7624.

Hayes, J. M., J. K. Gillie, D. Tang, and G. J. Small. 1988. Theory for spectral hole burning of the primary electron donor state of photosynthetic reaction centers. *Biochim. Biophys. Acta.* 932:287–305.

Hayes, J. M., R. Jankowiak, and G. J. Small. 1987. Two-level-system relaxation in amorphous solids as probed by nonphotochemical hole-burning in electronic transitions. *In* Topics in Current Physics, Persistent Spectral Hole Burning: Science and Applications. W. E. Moerner, editor. Springer Verlag, New York. 153–202.

Henderson, B. W., and T. J. Dougherty. 1992. How does photodynamic therapy work? *Photochem. Photobiol.* 55:145–157.

Jankowiak, R., R. S. Cooper, D. Zamzow, G. J. Small, G. Doskocil, and A. M. Jeffrey. 1988. Fluorescence line narrowing-hole burning spectrometry: femtomole detection and high selectivity for intact DNA-PAH adducts. *Chem. Res. Toxicol.* 1:60–68.

Jankowiak, R., J. M. Hayes, and G. J. Small. 1993. Spectral hole-burning spectroscopy in amorphous molecular solids and proteins. *Chem. Rev.* 93:1471–1502.

Jankowiak, R., and G. J. Small. 1987. Hole-burning spectroscopy and relaxation dynamics of amorphous solids at low temperatures. *Science.* 237:618–625.

Jankowiak, R., and G. J. Small. 1991. Fluorescence line narrowing: a high-resolution window on DNA and protein damage from chemical carcinogens. *Chem. Res. Toxicol.* 4:256–269.

Jankowiak, R., and G. J. Small. 1993. Spectral hole burning: a window on excited state electronic structure, heterogeneity, electron-phonon coupling, and transport dynamics of photosynthetic units. *In* The Photosynthetic Reaction Center. J. Diesenhofer and J. Norris, editors. Academic, New York. 133–177.

Kador, L., D. Haarer, and R. Personov. 1987. Stark effect of polar and unpolar dye molecules in amorphous hosts, studied via persistent spectral hole burning. *J. Chem. Phys.* 86:5300–5307.

Kaposi, A. D., J. Fidy, S. S. Stavrov, and J. M. Vanderkooi. 1993. Optical fine structure investigation of porphyrin-protein interactions: magnesium and metal-free myoglobin. *J. Phys. Chem.* 97:6319–6327.

Kenney, M., R. Jankowiak, and G. J. Small. 1990. Dispersive kinetics of nonphotochemical hole growth of oxazine 720 in glycerol, polyvinyl alcohol and their deuterated analogues. *Chem. Phys.* 146:47–61.

Kim, W.-H., T. Reinot, J. M. Hayes, and G. J. Small. 1995. Hyperquenched glassy films of water: a study by hole burning. *J. Phys. Chem.* 99: 7300–7310.

Kim, W.-H., T. Reinot, J. M. Hayes, and G. J. Small. 1996. Nonphotochemical hole burning in hyperquenched glassy films of water: a pronounced deuteration effect. *J. Chem. Phys.* 104:6415–6417.

Laird, B. B., and J. L. Skinner. 1989. Microscopic theory of reversible pressure broadening in hole-burning spectra of impurities in glasses. *J. Chem. Phys.* 90:3274–3281.

Meixner, A. J., A. Renn, S. E. Bucher, and U. P. Wild. 1986. Spectral hole burning in glasses and polymer films: the Stark effect. *J. Phys. Chem.* 90:6777–6785.

Milanovich, N., M. Suh, R. Jankowiak, G. J. Small, and J. M. Hayes. 1996. Binding of TO-PRO-3 and TOTO-3 to DNA: fluorescence and hole burning studies. *J. Phys. Chem.* 100:9181–9186.

Moan, J., K. Berg, H. Anholt, and K. Madslien. 1994. Sulfonated aluminum phthalocyanines as sensitizers for photochemotherapy. Effects of small light doses on localization, dye fluorescence and photosensitivity in V79 cells. *Int. J. Cancer.* 58:865–870.

Moerner, W. E., editor. 1987. Topics in Current Physics, Persistent Spectral Hole Burning: Science and Applications. Springer Verlag, New York. 153–202.

Peng, Q., G. W. Farrants, K. Madslien, J. C. Bommer, J. Moan, H. E. Danielsen, and J. M. Nesland. 1991. Subcellular localization, redistribution and photobleaching of sulfonated aluminum phthalocyanines in a human melanoma cell line. *Int. J. Cancer.* 49:290–295.

Reddy, N. R. S., R. Jankowiak, and G. J. Small. 1995. High-pressure hole-burning studies of the bacteriochlorophyll a antenna complex from *Chlorobium tepidum. J. Phys. Chem.* 99:16168–16178.

Reddy, N. R. S., P. A. Lyle, and G. J. Small. 1992. Applications of spectral hole burning spectroscopies to antenna and reaction center complexes. *Photosynth. Res.* 31:167–194.

Reinot, T., J. M. Hayes, and G. J. Small. 1997a. Electronic dephasing and electron-phonon coupling of aluminum phthalocyanine tetrasulphonate in hyperquenched and annealed glassy films of ethanol and methanol over a broad temperature range. *J. Chem. Phys.* 106:457–466.

Reinot, T., W.-H. Kim, J. M. Hayes, and G. J. Small. 1996. Electronic dephasing of APT in glassy films of water from 5 K to 100 K: implications for H-bonding liquids. *J. Chem. Phys.* 104:793–804.

Reinot, T., W.-H. Kim, J. M. Hayes, and G. J. Small. 1997b. A new standard for high-temperature persistent-hole-burning molecular materials: aluminum phthalocyanine tetrasulphonate in buffered hyperquenched glassy films of water. *J. Opt. Soc. Am. B.* 14:602–608.

Resnicoff, M., E. E. Medrano, O. L. Podhajcer, A. I. Bravo, L. Bover, and J. Mordoh. 1987. Subpopulations of MCF7 cells separated by Percoll gradient centrifugation: a model to analyze the heterogeneity of human breast cancer. *Proc. Natl. Acad. Sci. USA.* 84:7295–7299.

Rosenthal, I. 1991. Phthalocyanines as photodynamic sensitizers. *Photochem. Photobiol.* 53:859–870.

Schellenberg, P., J. Friedrich, and J. Kikas. 1994. Spectral hole burning in polymorphic systems: single site pressure phenomena and glassy behavior. *J. Chem. Phys.* 100:5501–5507.

Sesselman, Th., W. Richter, D. Haarer, and H. Morawitz. 1987. Spectroscopic studies of impurity-host interactions in dye-doped polymers: hydrostatic-pressure effects versus temperature effects. *Phys. Rev. B.* 36:7601–7611.

Shu, L., and G. J. Small. 1990. On the mechanism of nonphotochemical hole burning of optical transitions in amorphous solids. *Chem. Phys.* 141:447–455.

Shu, L., and G. J. Small. 1992a. Mechanism of nonphotochemical hole burning: cresyl violet in polyvinyl alcohol films. *J. Opt. Soc. Am. B.* 9:724–732.

Shu, L., and G. J. Small. 1992b. Dispersive kinetics of nonphotochemical hole burning and spontaneous hole filling: cresyl violet in polyvinyl films. *J. Opt. Soc. Am. B.* 9:733–737.

Shu, L., and G. J. Small. 1992c. Laser-induced hole filling: cresyl violet in polyvinyl alcohol films. *J. Opt. Soc. Am. B.* 9:738–745.

Small, G. J. 1995. On the validity of the standard model for primary charge separation in the bacterial reaction center. *Chem. Phys.* 197:239–257.

Soule, H. D., T. M. Maloney, S. R. Wolman, W. D. Peterson, Jr., R. Brenz, C. M. McGrath, J. Russo, R. J. Pauley, R. F. Jones, and S. C. Brooks. 1990. Isolation and characterization of a spontaneously immortalized human breast epithelial cell line, MCF-10. *Cancer Res.* 50:6075–6086.

Spikes, J. D. 1986. Phthalocyanines as photosensitizers in biological systems and for the photodynamic therapy of tumors. *Photochem. Photobiol.* 43:691–699.

Tait, L., H. D. Soule, and J. Russo. 1990. Ultrastructural and immunocytochemical characterization of an immortalized human breast epithelial cell line, MCF-10. *Cancer Res.* 50:6087–6094.

Wu, H.-M., S. Savikhin, N. R. S. Reddy, R. Jankowiak, R. J. Cogdell, W. S. Struve, and G. J. Small. 1996. Femtosecond and hole-burning studies of B800's excitation relaxation dynamics in the LH2 antenna complex of *Phodopseudomonas acidophila* (strain 10050). *J. Phys. Chem.* 100:12022–12033.

Zollfrank, J., J. Friedrich, J. Fidy, and J. M. Vanderkooi. 1991. Photochemical holes under pressure: compressibility and volume fluctuations of a protein. *J. Chem. Phys.* 94:8600–8604.